ARTICLE

Examining Nanoenvironments in Solids on the Scale of a Single, Isolated Impurity Molecule

W. E. Moerner*

Optical spectroscopy of single impurity molecules in solids can be used as an exquisitely sensitive probe of the structure and dynamics of the specific local environment around the single molecule (the "nanoenvironment"). Recently observed effects such as spectral diffusion, perturbations by external fields, changes in molecular photophysics, shifts in vibrational modes, optical modification of the absorption spectrum, dynamics due to amorphous system physics, and magnetic resonance of a single molecular spin attest to the vitality of and growing interest in this new field, which may lead to optical storage on the single-molecule level.

The power of high-resolution laser spectroscopy has recently been extended into the fascinating domain of individual impurity molecules in solids, where the single molecule acts as a probe of the detailed local environment of unprecedented sensitivity (*1–5*). In ongoing experiments at several laboratories around the world, exactly one molecule hidden deep within a solid sample is probed at a time by tunable laser radiation, which represents detection and spectroscopy of 1.66×10^{-24} moles of material, or 1.66 yoctomoles. Single molecule studies completely remove the normal ensemble averaging that occurs when a large number of molecules are probed at the same time. Thus, the usual assumption that all molecules contributing to the ensemble average are identical can now be directly examined, and strong tests of truly microscopic theories can be completed.

Single molecule spectroscopy (SMS) in solids is related to, but distinct from, the well-established field of sepectroscopy of single electrons, atoms, or ions confined in electromagnetic traps or on surfaces (*6–8*). The vacuum environment and confining fields of an electromagnetic trap are quite different from the environment of a single molecule in a solid where the lattice constrains the molecule, preventing rotation in most cases, and where the molecule is bathed in the phonon vibrations of the solid available at a given temperature. The near-field probing of atoms on surfaces with scanning tunneling microscopy or atomic force microscopy (*9*) usually requires a strong bond between the molecule of interest and the underlying surface as well as tolerance of the perturbing forces from the tunneling electrons or the tip. In contrast, SMS usually operates noninvasively in the optical far field with a corresponding loss in spatial resolution but with no loss of spectral resolution. In recent work, single-molecule imaging has been achieved with near-field optical techniques with 100-nm resolution at room temperature (*10, 11*). However, the spectral resolution that will be available under such conditions is three to four orders of magnitude poorer than the results of high-resolution SMS described here.

This article presents an overview of some of the recent advances produced by the spectroscopy of single impurity centers in solids, with emphasis on individual, isolated molecular impurities. One of several reviews may be consulted for more information (*4, 5*). These SMS studies are significant because (i) new physical effects have been observed in the single molecule regime and (ii) it is now possible in a single nanoenvironment to probe directly the connection between specific microscopic theories (*12*) of local structure, dynamics, and host-guest interactions and the statistical mechanical averages that are measured in conventional experiments.

How Single Molecule Spectroscopy in Solids Is Accomplished

One may ask: How is it possible to use optical radiation to isolate a single impurity molecule hidden deep inside a host matrix? There are several requirements necessary to ensure that the fluorescence emission from the molecule dominates over background signals (*13, 14*). First, only a small volume of sample on the order of a few hundred cubic micrometers is probed by the use of a thin sample and a small (micrometer-sized) laser spot produced by a lens, an optical fiber, or an aperture. In addition, the impurity concentration in the transparent host is low, in the range of 10^{-7} to 10^{-9} mol/mol. These two actions alone are insufficient to guarantee that only one impurity molecule in the probed volume is in resonance with the laser at a time. Additional selectivity on the order of a factor of 10^4 or so is provided by the careful selection of guest and host and the well-known properties of inhomogeneously broadened absorption lines in solids (*15–18*), summarized below.

For the usual case of detection by fluorescence excitation, the quantum yield for photon emission per absorption event should be high. A further requirement on the guest species stems from the photophysics of optical absorption in solids. The probability that a single molecule will absorb a photon from the incident beam is simply σ_{pk}/A, where σ_{pk} is the peak absorption cross section and A is the area of the laser beam. It has been recognized since the first SMS experiments that to produce ab-

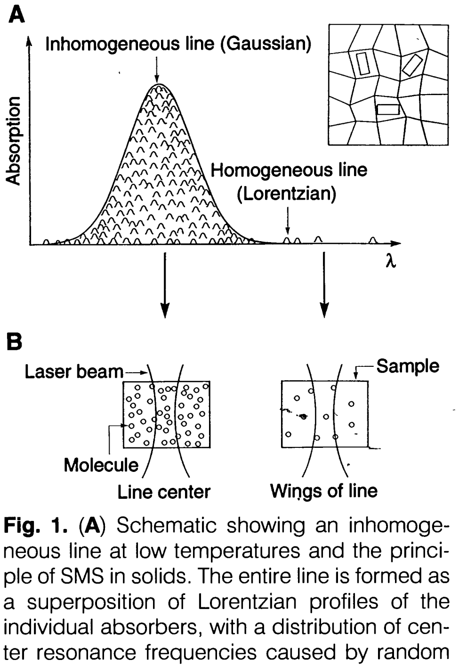

Fig. 1. (**A**) Schematic showing an inhomogeneous line at low temperatures and the principle of SMS in solids. The entire line is formed as a superposition of Lorentzian profiles of the individual absorbers, with a distribution of center resonance frequencies caused by random strains and imperfections. In the inset, several dopant molecules are sketched with different nanoenvironments. (**B**) Controlling the number of impurity molecules in resonance in the probed volume by changing the laser wavelength. The laser linewidth is negligible on the scale shown.

The author is at the IBM Research Division, Almaden Research Center, 650 Harry Road, K13/801, San Jose, CA 95120–6099, USA, and Laboratory of Physical Chemistry, Swiss Federal Institute of Technology, Universitätstrasse 22, CH-8092, Zürich, Switzerland.

*Present address: IBM Research Division, Almaden Research Center, 650 Harry Road, K13/801, San Jose, CA 95120–6099, USA.

sorption events efficiently with the incident photons rather than unwanted scattering signals, σ_{pk} should be as large as possible (*1, 14, 19–21*). Because σ_{pk} depends linearly upon the oscillator strength and inversely upon the optical homogeneous linewidth, $\Delta\nu_H$, strong absorptions and narrow lines give the largest σ_{pk} values. Strong absorptions are conveniently provided by electric-dipole–allowed, singlet-singlet transitions in aromatic molecules where the oscillator strength is often near unity. The narrowest optical linewidths in solids occur for zero-phonon, zero-vibration electronic transitions at low temperatures, because such transitions can only broaden by phonon scattering. For rigid molecules like pentacene or perylene in a solid below 10 K, the linewidth of the optical transition near 500 THz is on the order of 10 MHz, and σ_{pk} reaches values near 10^{-11} cm^2, thousands of times the area of a single molecule.

There is an additional crucial effect important for SMS resulting from the extreme narrowness of zero-phonon transitions: inhomogeneous broadening (*15, 16*) (see Fig. 1, top). This effect occurs when $\Delta\nu_H$ becomes narrower than the (mostly static) distribution of resonance frequencies in the solid caused by dislocations, point defects, or random internal strain and electric fields and field gradients (inset). Inhomogeneous broadening is a universal feature of high-resolution optical spectroscopy of defects in solids (*17, 18*), and of other spectroscopies in which zero-phonon lines are probed. (A dynamic inhomogeneous broadening also occurs for Doppler-broadened lines of gases.) Inhomogeneous broadening facilitates the selection of a single impurity, because the different guest molecules in the probe volume take on slightly different resonance frequencies according to the local fields at the location of the impurity. One then simply uses the tunability of a narrow-band laser to select different single-impurity centers. Naturally, this selection must be done in a region of the optical spectrum where the number of molecules per homogeneous width is on the order of or less than one. This may be accomplished by (i) tuning the laser wavelength out into the wings of the inhomogeneous line (Fig. 1, bottom right), (ii) using a sample with a very low doping level, or (iii) producing a large inhomogeneous linewidth; all three of these methods have been used.

A further requirement on the absorption properties of the probe molecule is the absence of strong bottlenecks in the optical pumping cycle. In organic molecules, intersystem crossing (ISC) from the singlet states into the triplet states represents a bottleneck, because photon emission usually ceases for a relatively long time equal to the triplet lifetime when ISC occurs. This effect results in premature saturation of the emission rate from the molecule and reduction of σ_{pk} compared to the case with no bottleneck (*22*). Thus, molecules with weak ISC yield and short triplet lifetime are preferable, such as rigid, planar aromatic dyes.

A final requirement for SMS is the selection of a guest-host couple that allows for the photostability of the impurity and weak spectral hole-burning. By this spectral hole-burning, we include any light-induced change in the resonance frequency of the molecule caused either by photochemistry of the molecule or by a photophysical change in the nearby environment (*23*). For example, most detection schemes with overall photon collection efficiency of 1 to 0.1% require that the quantum efficiency for hole-burning, η, be less than 10^{-6} to 10^{-7}. This requirement is necessary to provide sufficient time-averaging of the single molecule line shape before it changes appreciably or shifts to another spectral position.

All of these concepts may be used to derive specific expressions for the signal-to-noise ratio (SNR) for SMS (*4, 24*), and values on the order of 20 can be expected with 1-s integration time and spot diameters of a few micrometers for a system like pentacene impurities in a *p*-terphenyl crystal. To date, SMS has been achieved in four host-guest combinations with the three impurity molecules shown in Fig. 2: pentacene in *p*-terphenyl crystals (*1*), perylene in poly(ethylene) (*25*), terrylene in poly(ethylene) (*26*), and quite recently, terrylene in the Shpol'skii matrix hexadecane (*27*). The Shpol'skii matrices in particular should provide a large new class of materials that allow SMS.

Examples of Single Molecule Spectra

Fluorescence excitation spectra for a 10-μm-thick sublimed crystal of pentacene in *p*-terphenyl at 1.5 K are shown in Fig. 3 [for specific details of the experimental apparatus, see (*13*)]. In this method, the optical absorption is measured by recording the total fluorescence emission shifted to long wavelengths as the laser frequency is scanned over the resonance. The 18-GHz spectrum in Fig. 3A (obtained by the scan-

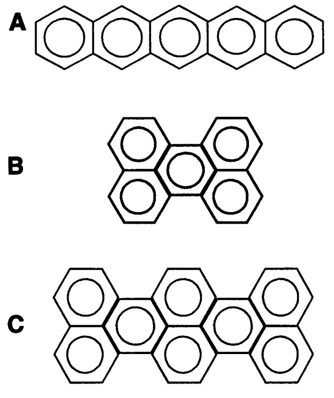

Fig. 2. Structures of molecules used so far for SMS: (**A**) pentacene, (**B**) perylene, and (**C**) terrylene.

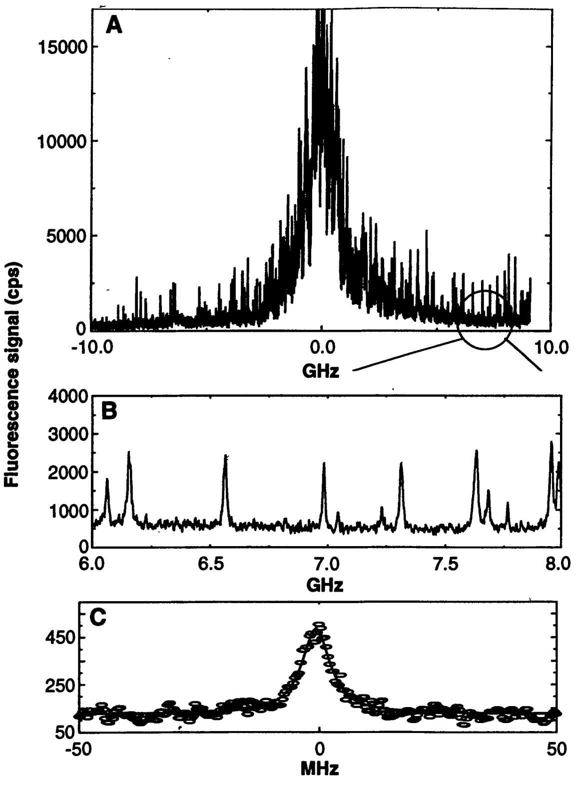

Fig. 3. Fluorescence excitation spectra for pentacene in *p*-terphenyl at 1.5 K. (**A**) Broad scan of the inhomogeneously broadened line; all the spikes are repeatable features. (**B**) Expansion of a 2-GHz region [area circled in (A)] showing several single molecules. The laser detuning is referenced to the line center at 592.321 nm. (**C**) Low-power scan of a single molecule at 592.407 nm showing the lifetime-limited width of 7.8 MHz and a Lorentzian fit; cps, counts per second.

ning of a 3-MHz linewidth dye laser over the entire inhomogeneous line) contains 20,000 points; to show all the fine structure usually requires several meters of linear space. The structures appearing to be spikes are not noise; all features shown are static and repeatable. Near the center, the "spectral roughness" is a fundamental effect called statistical fine structure (SFS) (*28, 29*) which arises directly from statistical variations in the spectral density of resonance frequencies. It is immediately obvious that the inhomogeneous line is far from Gaussian in shape and that there are tails extending out many standard deviations both to the red and to the blue. Figure 3B shows an expanded region in the wing of the line. Each of the narrow peaks is the absorption line of a single molecule. The different molecules have slightly different peak heights because the laser transverse intensity profile is bell-shaped and the molecules are not all located at the center of the focal spot. Although these spectra seem narrow, they are in fact slightly power-broadened by the probing laser.

Upon the close examination of an individual single-molecule peak at lower intensity (Fig. 3C), the quantum-limited linewidth of 7.8 ± 0.2 MHz can be observed (*30*). Here, the quantum limit applies because the optical linewidth has reached the minimum value allowed by the lifetime of the optical excited state. This value is in excellent agreement with previous photon echo measurements of $\Delta\nu_H$ using large ensembles of pentacene molecules (*31, 32*). In summary, it is clear that well-isolated single molecule spectra like those in Fig. 3 allow many spectroscopic studies of the local environment to be performed, because such narrow lines are much more sensitive to local perturbations than are broad spectral features.

Historical Background and Summary of Results

The foundations for SMS were laid in 1987 when the SFS signal scaling as the square root of the number of absorbers was first observed (*28, 29*) for pentacene in *p*-terphenyl. The first single molecule spectra were also recorded in this model system with a sophisticated zero-scattering-background absorption technique, FM spectroscopy, and either Stark or ultrasonic strain modulation of the absorption line (*1, 2*). The SNR in these experiments of about 5:1 was limited by the shot noise of the laser. In 1990, Orrit and Bernard demonstrated that fluorescence excitation produces superior signals if the emission is collected efficiently and if the scattering sources are minimized (*3*). Subsequent experiments have used fluorescence excitation exclusively.

For example, with SMS methods it has been possible to observe the quantum-limited linewidth of a single molecule (*30*), temperature-dependent dephasing (*13*), optical saturation (*13*), the effects of applied electric fields in crystals (*33*) and polymers (*26*), and shifts caused by external hydrostatic pressure (*34*), all of which represent applications of the tools of the spectroscopist to the narrow spectral line of a single molecule in a solid at low temperatures. With a proper time-delayed photon counting apparatus, the fluorescence emission lifetime of a single molecule can be directly measured (*35*). More surprisingly, several unexpected effects have also been observed, including the spectral diffusion of a single molecule due to dynamics of the nearby host (*36*), reversible optical modification that could lead to optical storage on a single molecule scale (*24, 25*), and even magnetic resonance of a single molecular spin (*37–39*). The correlation properties of the emitted photons have been used to good advantage to measure the photophysics of single molecules (*40*), resonance frequency fluctuations due to host degrees of freedom (*41*), and a quantum-optical effect, photon antibunching (*42*). It has also been possible to obtain fairly detailed information about the nanoenvironment of a single molecule by the measurement of the vibrational mode properties in the electronic ground state (*43–45*).

Imaging Single Molecules in Solids

As a survey of some specific SMS studies, Fig. 4 shows a three-dimensional "image" of single molecules in a solid first obtained for pentacene in *p*-terphenyl some years ago (*13*). The *z* axis of the image is the usual fluorescence signal, the horizontal axis is the laser frequency detuning (300-MHz range), and the axis going into the page is one transverse spatial dimension (40-μm range). The spatial scan is produced by slowly translating the laser focal spot across the face of the crystal and obtaining spectra at each position. There are three large, clear, single molecule peaks localized in both frequency and position at the center, upper left, and upper right. The spatial resolution of this image is clearly limited by the 5-μm-diameter laser spot; however, in the frequency dimension, the features are fully resolved.

The frequency widths of the peaks in Fig. 4 are slightly larger than the lifetime-limited width (Fig. 3C) because of the use of higher probing intensity. The oddly shaped peak between the two strong molecules at the center and upper right results from a molecule that is spectrally diffusing because of changes in its local nanoenvironment during the measurement (see the next section).

In recent work at ETH-Zürich, four-dimensional images have been obtained for pentacene in *p*-terphenyl with two spatial and one frequency dimension as well as the signal dimension (*46*). This "fluorescence microscopy" experiment used an image intensifier–video camera combination specifically configured as a photon counter in each pixel. Single molecules resemble star-like objects that appear and disappear as the laser frequency is scanned. Future work in this area may increase the spatial resolution by near-field optical techniques (*10*). At low temperatures, the narrowness of the spectral features compared to room temperature should provide unprecedented detail of the local environment of the impurity molecule.

Direct Observations of Spectral Diffusion and Host Dynamics

When a new regime is first opened for study, new physical effects can often be observed. In the course of the early SMS of pentacene in *p*-terphenyl, an unexpected phenomenon appeared: resonance frequency shifts of individual pentacene molecules in a crystal at 1.5 K (*36*), called spectral diffusion by analogy to amorphous systems (*47*). Here, spectral diffusion means changes in the center (resonance) frequency of a defect due to configurational changes in the nearby host

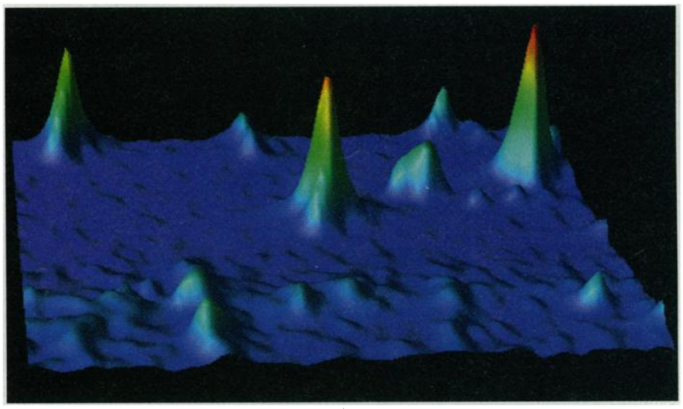

Fig. 4. Three-dimensional "images" of single molecules. The measured fluorescence signal (*z* axis) is displayed over a range of 300 MHz in excitation frequency near 592.544 nm (horizontal axis) and 40 μm in spatial position (axis into the page). (Rendered with IBM Data Explorer, San Jose, California.)

that affect the frequency of the electronic transition through guest-host coupling. Experimentally, two distinct classes of single pentacene molecules were identified: class I molecules, which have center frequencies that were stable in time like the three large molecules in Fig. 4, and class II molecules, which showed spontaneous, discontinuous jumps in resonance frequency of 20 to 60 MHz on a 1- to 420-s time scale, which are responsible for the distorted single-molecule peak in Fig. 4.

To illustrate the behavior of the type II molecules, Fig. 5A shows a sequence of excitation spectra of a single molecule taken as fast as allowed by the available SNR. The laser was scanned once every 2.5 s with 0.25 s between scans, and the hopping of this molecule from one resonance frequency to another is clearly evident. By acquiring hundreds to thousands of such spectra, a trajectory or trend of the resonance frequency can be obtained (Fig. 5B, for the same molecule as Fig. 5A). For this molecule, the optical transition energy appears to have a preferred set of values and performs spectral jumps between these values that are discontinuous on the 2.5-s time scale of the measurement. The behavior of another molecule is shown in Fig. 5C at 1.5 K and in Fig. 5D at 4.0 K. This molecule wanders in frequency space with many smaller jumps, and both the rate and range of spectral diffusion increase with temperature, suggesting a phonon-driven process. The occurrence of class II molecules was quite common in the wings of the inhomogeneous line, but only class I molecules were observed close to the center, suggesting a connection to disorder in the crystal structure. In addition, the jumping rate did not depend on the probing laser power. The spectral diffusion appeared to be a spontaneous process rather than a light-induced, spectral hole-burning effect (*30*).

Because the optical absorption is highly polarized (*48*) and the peak signal from the molecule does not decrease when the spectral jumps occur, it is unlikely that the molecule is changing orientation in the lattice. Because the resonance frequency of a single molecule in a solid is extremely sensitive to the local strain, the conclusion is that the spectral jumps are due to internal dynamics of some configurational degrees of freedom in the surrounding lattice. The situation is analogous to that for amorphous systems, which are postulated to contain a multiplicity of local configurations that can be modeled by a collection of double-well potentials [the two-level system, or TLS, model (*49*)]. The dynamics result from phonon-assisted tunneling or thermally activated barrier-crossing in these potential wells. One possible source for the tunneling states (*13*) could be discrete torsional librations of the central phenyl ring of the nearby *p*-terphenyl molecules about the molecular axis. The *p*-terphenyl molecules in a domain wall between two twins or near lattice defects may have lowered barriers to such central-ring tunneling motions. Further study is necessary to identify conclusively the specific molecular motions responsible for the effect. These direct observations of the dynamics of a nanoenvironment of a single molecule have sparked new theoretical studies of the underlying microscopic mechanism (*12*, *50*).

Spectral diffusion similar to that shown in Fig. 5 was also observed in SMS of perylene in poly(ethylene) (*24*, *25*) and of terrylene in poly(ethylene) (*26*, *51*). As opposed to the crystalline system, spectral diffusion is expected here (*47*) and is observed in a variety of time regimes. On the fast (sub-second) time scale, spectral shifts on the order of 10 to 100 MHz produce single-molecule line shapes that fluctuate from measurement to measurement. On longer time scales, jumping behavior can be observed that is similar to that shown in Fig. 5B. Detailed measurements of terrylene in poly(ethylene) (*51*) also suggest that at higher laser powers, more spectral diffusion is observed that may be regarded as a type of transient spectral hole-burning. Orrit and colleagues (*41*, *52*) have used photon correlation techniques to study such processes.

These measurements of spectral diffusion in crystals and polymers illustrate the power of SMS in detecting changes in the nanoenvironment of a single molecule. The spectral changes can be followed in real time for each impurity molecule; no ensemble averages over "equivalent" centers need be made that would obscure the effects.

Fig. 5. Examples of single molecule spectral diffusion for pentacene in *p*-terphenyl at 1.5 K. (**A**) A series of fluorescence excitation spectra each 2.5 s long spaced by 2.75 s showing discontinuous shifts in resonance frequency, with zero detuning at 592.546 nm. (**B**) Trend or trajectory of the resonance frequency over a long time scale for the molecule in (A). (**C**) Resonance frequency trend for a different molecule at 592.582 nm at 1.5 K and (**D**) at 4.0 K.

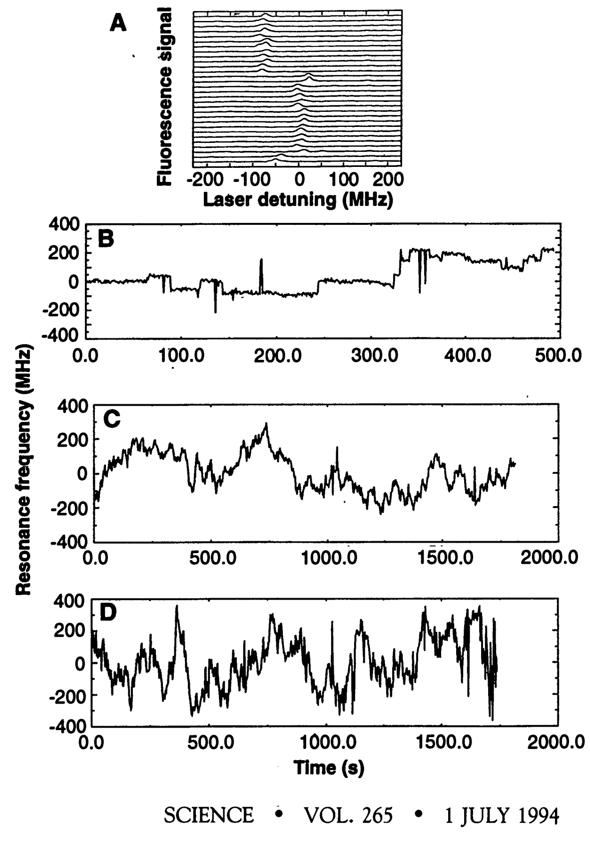

Optical Modification of Single Molecule Spectra: Applications to Optical Storage

A spectral hole usually refers to a dip in the inhomogeneously broadened absorption spectrum of many molecules when light irradiation alters the absorption frequencies of a portion of the resonant absorbers (*23*). In the single molecule regime, however, only the isolated absorption line of one center is present. When photochemical or photophysical changes occur as a result of optical excitation, the absorption line simply appears to vanish as the resonance frequency of the single center shifts away from the laser frequency. Because laser-induced resonance frequency shifts form the foundation for the spectral hole-burning process, I will continue to use the term "hole-burning" even for the single molecule case.

At first glance, the spontaneous spectral diffusion of the last section seems similar to single molecule hole-burning, and in some cases it may be hard to distinguish the two (*51*), because when a single molecule changes resonance frequency, one may not know which mechanism produced the change. Because hole-burning is driven by the light and does not spontaneously occur as the spectral diffusion of the last section, one must observe a dependence on the laser intensity to verify that hole-burning is occurring. The exact microscopic mechanism for light-induced resonance frequency shifts needs further study and may be related to the generation of molecular internal vibrational modes during fluorescence emission or to nonradiative decay of the excited state.

This effect was first convincingly observed for perylene in poly(ethylene) (*24, 25*), where a clear increase in hole-burning rate could be observed at higher laser power because the single molecules showed reversible hole-burning. Here, reversibility means the spontaneous return of the resonance frequency to its original value after hole-burning, which allowed many measurements of the stochastic burning-time kinetic distribution for the same molecule (*25*). Irreversible hole-burning was also observed, and Fig. 6 illustrates this effect for a spectral region containing four different molecules. Starting from the bottom, the first 10 traces show that the molecule near +2 GHz is spectrally diffusing while the other three molecules are relatively stable with a small amount of spectral diffusion. After trace 10, the laser was deliberately brought into resonance with the molecule at 0.5 GHz, which was observed to stop fluorescing discontinuously after ≅28 s, indicating the hole-burning. Trace 11 was then recorded, which shows that the molecule shifted its resonance frequency outside of the laser scan range. The remaining traces show that the molecule did not return to its original frequency for at least 15 min. The exact location of the new resonance frequency was unknown, but by analogy with previous nonphotochemical hole-burning studies on large ensembles (*53, 54*), the shift could have been as large as 100 cm^{-1}. In recent work on the new system of terrylene in hexadecane (*55*), well-defined two-state switching behavior was observed that could be partially controlled by the laser irradiation.

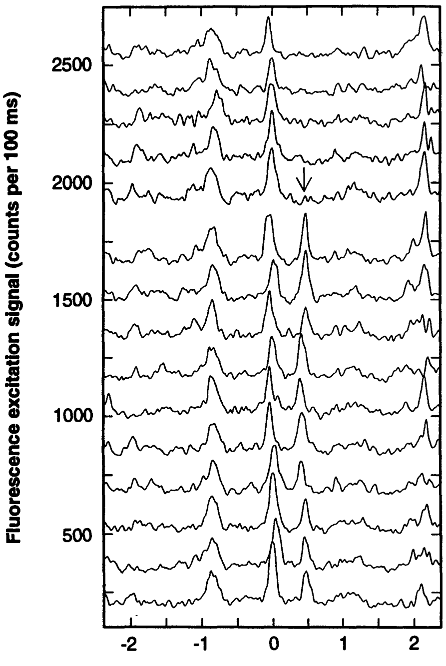

Fig. 6. Persistent spectral hole-burning of a single perylene in polyethylene arbitrarily chosen out of four molecules in a 4.6-GHz scan range (T = 1.5 K, 0 GHz detuning at 448.019 nm). The burning event for the molecule at 0.5 GHz (arrow) was executed after the tenth trace counting from the bottom or in terms of time 29 min after the first trace shown [Adapted from (*24*)].

In principle, single molecule hole-burning is a controllable process that could allow the modification of the transition frequency of any arbitrarily chosen molecule in the polymer host. This ability to change leads naturally to the possibility of optical storage at the single molecule level (Fig. 7). For highest density, near-field optical excitation with a 50-nm-diameter pulled fiber tip should be used, a process that has demonstrated densities of 45 gigabits per square inch with magneto-optic recording (*56*). One can imagine a thin layer of the material with a sufficiently broad inhomogeneous line so that single impurity molecules are isolated and spread over a large range of frequency space. The resonance frequencies constitute the addresses of all the bits to be written in a single focal volume. A binary sequence of 1's and 0's can be produced by altering or ignoring each single molecule absorption.

Single molecule optical storage, while highly speculative at present, provides several advantages and disadvantages. Among the advantages are (i) the extreme areal density (up to perhaps 10^{13} bits per square inch for a 50 nm by 50 nm storage volume and a doping level of 10^{-3}, giving 100 bits per spot), (ii) the increased signal from each molecule resulting from the use of sub–diffraction-limited beams, and (iii) the ease of access of different bits by the simple tuning of the laser. Some disadvantages are the required low temperatures, stochastically variable burning times, high doping level, and variable frequency locations of the individual bits from laser spot to laser spot. The last problem can be overcome in principle by "pre-formatting" the resonance frequencies or perhaps even by careful design of the inhomogeneous distribution. In spite of these problems, optical modification of single molecule spectra not only provides a unique window into the photophysics and low-temperature dynamics of the amorphous state, but it also allows such novel optical storage schemes to be studied and developed.

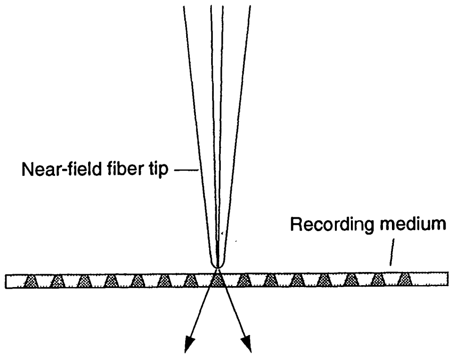

Fig. 7. Illustration of possible scheme for ultrahigh density optical storage with the use of light-induced spectral modification of single molecules and near-field optics. In each cross-hatched volume, many bits are recorded with the use of single molecules at different positions in the inhomogeneous line.

Correlation of Photons Emitted by a Single Molecule

The stream of photons emitted by a single molecule contains information about the system encoded in the arrival times of the individual photons. Figure 8 schematically shows the time domain behavior of the photon stream for a single molecule with a dark triplet state, here taken to be pentacene. While cycling through the singlet states of $S_0 \leftrightarrow S_0$, photons are emitted until intersystem crossing occurs. Because the triplet yield is 0.5% (*57*), 200 photons are emitted on average before a dark period that has an average length equal to the triplet lifetime, τ_T. This effect causes "bunching" of the emitted photons, as shown in the upper half of Fig. 8. The subsequent decay in the autocorrelation of the emitted photons for pentacene in *p*-terphenyl was reported by Orrit and Bernard (*3*), and this phenomenon has been used to measure distributions in the triplet yield and τ_T from molecule to molecule (*40*) resulting from distortions by the local nanoenvironment. Such correlation measurements can extract information on much shorter time scales (down to microseconds)

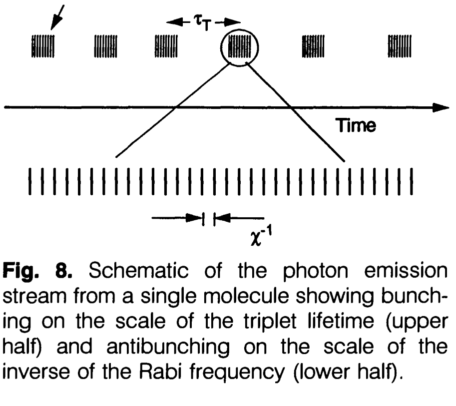

Fig. 8. Schematic of the photon emission stream from a single molecule showing bunching on the scale of the triplet lifetime (upper half) and antibunching on the scale of the inverse of the Rabi frequency (lower half).

than those of the frequency scans described above; however, the dynamical process under study must be "stationary," that is, it must not change during the many seconds needed to record a valid autocorrelation. For terrylene in poly(ethylene), which has complex dynamics driven by TLSs in the polymer, the amplitude fluctuations in the single-molecule fluorescence signal resulting from resonance frequency shifts sometimes cause a characteristic falloff in the autocorrelation that yields information about the TLS-phonon coupling (*41, 52*).

By contrast, in the nanosecond time regime (lower half of Fig. 8), the emitted photons from a single quantum system are expected to show antibunching, which means that the photons "space themselves out in time;" that is, the probability for two photons to arrive at the detector at the same time is small. This is a quantum-mechanical effect, which was first observed for sodium atoms in a low-density beam (*58*). For a single molecule, antibunching is easy to understand: After photon emission, the molecule is definitely in the ground state and cannot emit a second photon immediately. A time on the order of the inverse of the Rabi frequency, χ^{-1}, must elapse before the probability of emission of a second photon is appreciable. Antibunching for a single molecule was observed at IBM for pentacene in *p*-terphenyl (*42*), demonstrating that quantum optics experiments can be performed in solids and with a single molecule. Of course, if more than one molecule is emitting, the antibunching effect as well as the bunching effect quickly disappears because the molecules emit independently. Thus, high-contrast anti-bunching is further proof that the spectral features are indeed those of single molecules.

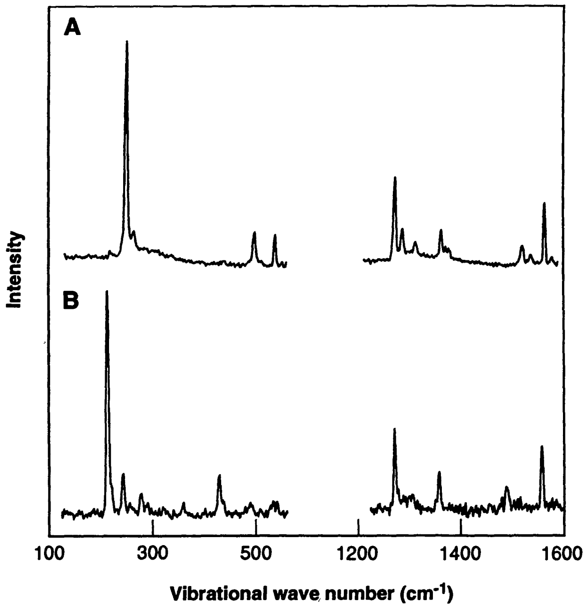

Fig. 9. Examples of dispersed fluorescence spectra showing vibrational mode frequencies and intensities for two molecules of terrylene in poly(ethylene). (**A**) Molecule probably located in a crystalline region (laser wavelength = 577.19 nm). (**B**) Molecule probably located in an amorphous region (laser wavelength = 572.46 nm).

Vibrational Modes of Single Molecules

Until recently, all SMS studies used the total fluorescence excitation technique in which all long-wavelength–shifted photons passing through a long-pass filter are recorded. With the use of a grating spectrograph and a charge-coupled device array detector, vibrationally resolved emission spectra from single molecules both in crystals (*43*) and in polymers (*44, 45*) have been obtained. Such experiments may also be regarded as resonance Raman studies, because the laser is in resonance with the 0-0 electronic transition, and even-parity vibrational modes of the ground state are detected by the measurement of the shift between the laser wavelength and the wavelength of the emission peak. The ability to examine vibronic or vibrational features of individual absorbers can generate much more detail about the identity of the absorber and the nature of the interactions with the nanoenvironment which produce shifts or intensity changes in the vibrational spectrum.

Typical dispersed fluorescence spectra for two different single molecules of terrylene in poly(ethylene) at 1.6 K are shown in Fig. 9. In addition to small ($\cong$cm^{-1}) shifts and intensity changes of various modes from molecule to molecule, two different classes of spectra were observed (*44*), as shown in the upper and lower parts of the figure. After considering various possibilities, the investigators concluded that the upper type of spectrum resulted from a terrylene molecule on the surface of or inside the crystalline lamellae of the polymer, while the other spectrum resulted from a single terrylene located in an amorphous region. Such results demonstrate the wealth of spectroscopic detail that can be obtained from individual molecules to probe truly local aspects of the structure of amorphous solids. For example, the lowest frequency mode in Fig. 9 is a long axis ring expansion of the molecule; the shift to lower energy in the amorphous site can be understood as resulting from the reduced local density (greater free volume) compared to the crystalline site. Such measurements will stimulate new theoretical calculations of the spectral changes that result from specific local distortions for comparison with the single molecule spectra.

Magnetic Resonance of a Single Molecular Spin

Historically, the standard methods of electron paramagnetic resonance and nuclear magnetic resonance have been limited in sensitivity to about 10^8 electron spins and about 10^{15} nuclear spins, respectively, due chiefly to the weak interaction between the individual spins and the radio-frequency electromagnetic fields used for detection. Using a combination of SMS and optically detected magnetic resonance (ODMR), two research groups have independently observed the magnetic resonance transition of a single molecular spin (*37, 38*) using the pentacene in *p*-terphenyl model system. In essence, ODMR allows higher sensitivity because the weak spin transition is effectively coupled to a much stronger optical transition with oscillator strength near unity. The method involves selecting a single molecule with the laser as described above and monitoring the intensity of optical emission (here, fluorescence from the first excited singlet state) as the frequency of a microwave signal is scanned over the frequency range of the triplet spin sublevel splittings (*59*). Because the emission rate is dependent on the overall lifetime of the triplet (bottleneck) state, the emission rate is affected when the microwave frequency is resonant with transitions among the triplet spin sublevels.

Figure 10 shows examples of the 1480-MHz magnetic resonance transition among the T_x to T_z triplet-spin sublevels at 1.5 K for a single molecule of pentacene in *p*-terphenyl, where the signal plotted is the change in the fluorescence emission rate as a function of the applied microwave frequency (*37*). Traces A and B show the line shapes at large N when many pentacene molecules are pumped by the laser, where O_1 and O_2 refer to the specific substitutional sites for pentacene in the host. Traces C to G show the line shapes for four different single molecules. As is the case for large N, the line shape of the ODMR transition for a single spin is broadened by hyper-fine interactions with nearby proton nuclear spins. This broadening occurs because many different configurations of the protons in the molecule are sampled on the time scale of the measurement of the triplet state transition. In contrast, in the large N experiment an ensemble average is measured rather than a time average.

These observations open the way for a variety of new studies of magnetic interactions in solids at the level of a single molecular spin, such as the use of external magnetic fields to reduce proton spin flips and hence the hyper-fine broadening. Already single spin coherence has been observed (39), because no matter what time the molecule enters the triplet state, the start of the microwave irradiation provides a zero-time reference so that the signals from subsequent entries into the triplet can add coherently. In future work, the properties of amorphous organic materials may be studied in greater detail, as the selection of a single molecular spin removes all orientational anisotropy as well as all inhomogeneous broadening. Imaging on the spatial scale of a single molecule is possible with a sufficiently large magnetic field gradient. The power of magnetic resonance in general in the study of fine and hyper-fine interactions, local structure, and molecular bonding can now be enhanced with these first demonstrations of useful sensitivity in the single spin regime.

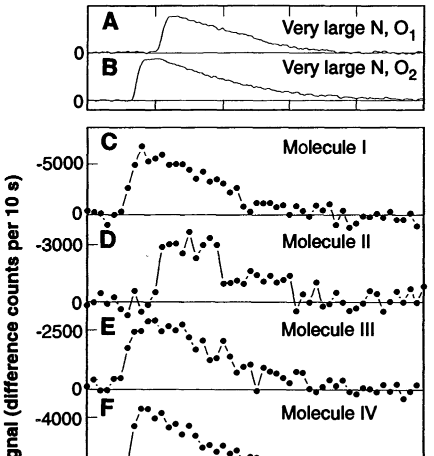

Fig. 10. Single-spin magnetic resonance for pentacene in *p*-terphenyl at 1.5 K. The fluorescence detected magnetic resonance (FDMR) signal is shown as a function of the microwave frequency applied to the sample. (**A** and **B**) The T_x to T_z transition for a large number of molecules for sites O$_1$ and O$_2$. (**C** to **G**) A selection of single-molecule magnetic resonance line shapes [adapted from (*37*)].

Outlook

The attainment of SMS in solids opens up a new frontier of single-absorber experiments in which the measured properties of the absorbing center are not averaged over many "equivalent" absorbers. The significance of such experiments is fourfold. First, the properties of a single absorber are measured without ensemble averaging, which means that tests of specific theoretical models are much stronger. Second, the sensitivity to specific properties of the nanoenvironment such as the local phonon modes and the true local fields is extremely high. This sensitivity means, for example, that the identity of the mysterious two-level systems in amorphous materials may finally be determined. Third, it provides a window into the spectral hole-burning process on a molecule by molecule basis. Thus, the exact local coupling through which optical pumping of a single molecule gives rise to changes in the nanoenvironment that shift the resonance frequency may be studied. Fourth, this regime is essentially unexplored, which means that surprises and unexpected physical effects can occur (such as the observation of spectral diffusion in a crystal).

While as a general technique SMS is not applicable to all molecular impurities, it can be applied to the large number of absorbing molecules (and perhaps ions) in solids that have zero-phonon transitions, reasonable absorption strength, and efficient fluorescence. The detectability of the resulting single-center signal, which ultimately depends on the specific sample and weak or absent spectral hole-burning, must be evaluated in each case. Single-molecule excitation spectra should be observable at higher and higher temperatures if the concentration and background are both reduced sufficiently. One method for making this reduction may be to use near-field excitation (*10, 11*) to reduce the scattering volume and increase the single center signal.

Other future experiments may be contemplated. Detailed study of the spectral diffusion process in crystals and polymers will help eventually to identify the actual microscopic nature of the two-level systems. Nonlinear spectroscopy to measure the ac Stark effect for a single isolated molecule may also be performed. With the proper choice of lifetimes, quantum jumps and other processes observed for single ions in vacuum electromagnetic traps would be expected to become directly observable. The door is also open to true photochemical experiments on single absorbers at low temperatures and even the possibility of optical storage with the use of single molecules. Future efforts to increase the number of probe-host couples that allow single-molecule spectra will lead to an even larger array of possibilities.

One novel experiment that is now possible would be to use the emission from a single molecule as a light source of subnanometer dimensions for near-field optical microscopy (60). Of course, this experiment would involve the technical difficulty of placing the single molecule at the end of a pulled fiber tip. Another possibility would be to perform cavity quantum electrodynamics studies with a single molecule in a solid placed in a high-Q (quality factor, or the center frequency of the cavity/the linewidth of the cavity resonance) cavity. In all cases, improvements in SNR would be expected to open up a new level of physical detail and possibly new applications for this method. Because this field is relatively new, the possibilities are only limited at present by the imagination and the persistence of the experimenter and the continuing scientific interest in the properties of single quantum systems in solids.

REFERENCES AND NOTES

1. W. E. Moerner and L. Kador, *Phys. Rev. Lett.* **62**, 2535 (1989).
2. L. Kador, D. E. Horne, W. E. Moerner, *J. Phys. Chem.* **94**, 1237 (1990).
3. M. Orrit and J. Bernard, *Phys. Rev. Lett.* **65**, 2716 (1990).
4. W. E. Moerner and Th. Basché, *Angew. Chem.* **105**, 537 (1993); *Angew. Chem. Int. Ed. Engl.* **32**, 457 (1993).
5. M. Orrit, J. Bernard, R. Personov, *J. Phys. Chem.* **97**, 10256 (1993).
6. W. M. Itano, J. C. Bergquist, D. J. Wineland, *Science* **237**, 612 (1987), and references therein.
7. F. Diedrich, J. Krause, G. Rempe, M. O. Scully, H. Walther, *IEEE J. Quantum Electron.* **24**, 1314 (1988), and references therein.
8. H. Dehmelt, W. Paul, and N. F. Ramsey, *Rev. Mod. Phys.* **62**, 525 (1990).
9. G. Binnig and H. Rohrer, *ibid.* **59**, 615 (1987).
10. E. Betzig and R. J. Chichester, *Science* **262**, 1422 (1993).
11. W. P. Ambrose, P. M. Goodwin, J. C. Martin, R. A. Keller, *Phys. Rev. Lett.* **72**, 160 (1994).
12. P. D. Reilly and J. L. Skinner, *ibid.* **71**, 4257 (1993).
13. W. P. Ambrose, Th. Basché, W. E. Moerner, *J. Chem. Phys.* **95**, 7150 (1991).
14. W. E. Moerner, *J. Lumin.*, in press.
15. A. M. Stoneham, *Rev. Mod. Phys.* **41**, 82 (1969).
16. K. K. Rebane, *Impurity Spectra of Solids* (Plenum, New York, 1970), p. 99.
17. D. A. Wiersma, *Adv. Chem. Phys.* **47**, 421 (1981).
18. See *Laser Spectroscopy of Solids*, vol. 49 of *Springer Topics in Applied Physics*, W. M. Yen and P. M. Selzer, Eds. (Springer, Berlin, 1981).
19. W. E. Moerner and L. Kador, *Anal. Chem.* **61**, 1217A (1989).
20. W. E. Moerner, *New J. Chem.* **15**, 199 (1991).
21. K. K. Rebane and I. Rebane, *J. Lumin.* **56**, 39 (1993).
22. H. de Vries and D. A. Wiersma, *J. Chem. Phys.* **72**, 1851 (1980).
23. See *Persistent Spectral Hole Burning: Science and Applications*, vol. 44 of *Springer Topics in Current Physics*, W. E. Moerner, Ed. (Springer, Berlin, 1988).
24. Th. Basché, W. P. Ambrose, W. E. Moerner, *J. Opt. Soc. Am. B* **9**, 829 (1992).
25. Th. Basché and W. E. Moerner, *Nature* **355**, 335 (1992).
26. M. Orrit, J. Bernard, A. Zumbusch, R. I. Personov, *Chem. Phys. Lett.* **196**, 595 (1992).
27. T. Plakhotnik, W. E. Moerner, T. Irngartinger, U. P. Wild, *Chimia* **48**, 31 (1994).

28. W. E. Moerner and T. P. Carter, *Phys. Rev. Lett.* **59**, 2705 (1987).
29. T. P. Carter, M. Manavi, W. E. Moerner, *J. Chem. Phys.* **89**, 1768 (1988).
30. W. E. Moerner and W. P. Ambrose, *Phys. Rev. Lett.* **66**, 1376 (1991).
31. H. de Vries and D. A. Wiersma, *J. Chem. Phys.* **69**, 897 (1978).
32. F. G. Patterson, H. W. H. Lee, W. L. Wilson, M. D. Fayer, *Chem. Phys.* **84**, 51 (1984).
33. U. P. Wild, F. Güttler, M. Pirotta, A. Renn, *Chem. Phys. Lett.* **193** 451 (1992).
34. M. Croci, H.-J. Müschenborn, F. Güttler, A. Renn, U. P. Wild, *ibid.* **212**, 71 (1993).
35. M. Pirotta *et al.*, *ibid.* **208**, 379 (1993).
36. W. P. Ambrose and W. E. Moerner, *Nature* **349**, 225 (1991).
37. J. Köhler *et al.*, *ibid.* **363**, 242 (1993).
38. J. Wrachtrup, C. von Borczyskowski, J. Bernard, M. Orrit, R. Brown, *ibid.*, p. 244.
39. J. Wrachtrup, C. von Borczyskowski, J. Bernard, M. Orrit, R. Brown, *Phys. Rev. Lett.* **71**, 3565 (1993).
40. J. Bernard, L. Fleury, H. Talon, M. Orrit, *J. Chem. Phys.* **98**, 850 (1993).
41. A. Zumbusch, L. Fleury, R. Brown, J. Bernard, M. Orrit, *Phys. Rev. Lett.* **70**, 3584 (1993).
42. Th. Basché, W. E. Moerner, M. Orrit, H. Talon, *ibid.* **69**, 1516 (1992).
43. P. Tchénio, A. B. Myers, W. E. Moerner, *J. Phys. Chem.* **97**, 2491 (1993).
44. ———, *Chem. Phys. Lett.* **213**, 325 (1993).
45. A. B. Myers, P. Tchénio, W. E. Moerner, *J. Lumin.*, in press.
46. F. Güttler, T. Irngartinger, T. Plakhotnik, A. Renn, U. P. Wild, *Chem. Phys. Lett.* **217**, 393 (1994).
47. J. Friedrich and D. Haarer, in *Optical Spectroscopy of Glasses,* I. Zschokke, Ed. (Reidel, Dordrecht, the Netherlands, 1986), p. 149.
48. F. Güttler *et al.*, *J. Lumin.* **56**, 29 (1993).
49. See *Amorphous Solids: Low-Temperature Properties*, vol. 24 of *Springer Topics in Current Physics*, W. A. Phillips, Ed. (Springer, Berlin, 1981).
50. G. Zumofen and J. Klafter, *Chem. Phys. Lett.* **219**, 303 (1994).
51. P. Tchénio, A. B. Myers, W. E. Moerner, *J. Lumin.* **56**, 1 (1993).
52. L. Fleury, A. Zumbusch, M. Orrit, R. Brown, J. Bernard, *ibid.*, p. 15.
53. J. M. Hayes, R. P. Stout, G. J. Small, *J. Chem. Phys.* **74**, 4266 (1981).
54. R. Jankowiak and G. J. Small, *Science* **237**, 618 (1987).
55. W. E. Moerner, T. Plakhotnik, T. Irngartinger, M. Croci, V. Palm, U. P. Wild, *J. Phys. Chem.*, in press.
56. E. Betzig *et al.*, *Appl. Phys. Lett.* **61**, 142 (1992).
57. H. de Vries and D. A. Wiersma, *J. Chem. Phys.* **70**, 5807 (1979).
58. H. J. Kimble, M. Dagenais, L. Mandel, *Phys. Rev. Lett.* **39**, 691 (1977).
59. Effectively, the triplet state of the molecule is formed by two unpaired electrons with spin parallel to each other leading to a net electronic spin of 1. In zero external magnetic field, the triplet state splits into three spin sublevels because of the anisotropy of the molecular electronic wave function and the magnetic structure of the nearby environment.
60. K. Lieberman, S. Harush, A. Lewis, R. Kopelman, *Science* **247**, 59 (1990).
61. I thank W. P. Ambrose, Th. Basché, L. Kador, A. B. Myers, P. Tchénio, and U. P. Wild for fruitful collaborations.

RESEARCH ARTICLE

Stimulation of GAL4 Derivative Binding to Nucleosomal DNA by the Yeast SWI/SNF Complex

Jacques Côté, Janet Quinn, Jerry L. Workman,
Craig L. Peterson*

The SWI/SNF protein complex is required for the enhancement of transcription by many transcriptional activators in yeast. Here it is shown that the purified SWI/SNF complex is composed of 10 subunits and includes the SWI1, SWI2/SNF2, SWI3, SNF5, and SNF6 gene products. The complex exhibited DNA-stimulated adenosine triphosphatase (ATPase) activity, but lacked helicase activity. The SWI/SNF complex caused a 10- to 30-fold stimulation in the binding of GAL4 derivatives to nucleosomal DNA in a reaction that required adenosine triphosphate (ATP) hydrolysis but was activation domain-independent. Stimulation of GAL4 binding by the complex was abolished by a mutant SWI2 subunit, and was increased by the presence of a histone-binding protein, nucleoplasmin. A direct ATP-dependent interaction between the SWI/SNF complex and nucleosomal DNA was detected. These observations suggest that a primary role of the SWI/SNF complex is to promote activator binding to nucleosomal DNA.

The yeast SWI1, SWI2/SNF2, SWI3, SNF5, and SNF6 gene products are required for the induced expression of a large set of genes (*1*). Furthermore, SWI/SNF products are required for the enhancement of transcription by several gene-specific activator proteins in yeast, such as GAL4 (*2*), *Drosophila ftz* (*2*), mammalian glucocorticoid and estrogen receptors (*3*), and LexA-GAL4 and LexA-Bicoid fusion proteins (*4*). The SWI/SNF gene products function as components of a large multi-subunit protein complex of approximately 2 × 10^6 daltons (*5*, *6*). One activity of this complex is to associate with the mammalian glucocorticoid receptor (*3*). These observations suggested that homologs of the *SWI/SNF* genes would be present in *Drosophila* and mammals (*3*). Candidate homologs of the *SWI2* gene have been identified in *Drosophila* (*7*), mouse (*8*), and human (*9*, *10*). Protein chimeras between either BRG1 (one of two putative human homologs) or brahma (brm, the putative *Drosophila* homolog) and SWI2 are functional in yeast, which suggests that these relatives are functional homologs (*9*, *11*). Gel filtration data suggest that the BRG1 protein may also be a subunit of a large protein complex (*9*).

A current hypothesis of how the SWI/SNF complex facilitates activator function suggests that the complex antagonizes chromatin-mediated transcriptional repression. The relation between the SWI/SNF complex and chromatin structure was suggested because mutations in genes that encode chromosomal proteins alleviate the phenotypes of *swi* and *snf* mutants. Mutations that inactivate the *SIN1* gene, which encodes a putative nonhistone chromatin component, or in the *SIN2* gene, which encodes histone H3, alleviate the defects in growth and in transcription caused by mutations in

Table 1. Purification of the SWI/SNF complex was followed by protein immunoblots probing for the SWI2-HA-6HIS fusion protein. Similar levels of purification were obtained in at least four preparations.

	Volume (ml)	Concentration (mg/ml)	Total protein (mg)	Specific activity (units*)
WCE	130	21.5	2800	1
Ni^{2+} eluate	43	1	43	65
Mono Q	2	0.35	0.7	3,965
Superose	1.5	0.02	0.03	91,195

*One unit is equivalent to the amount of SWI2-HA-6HIS fusion protein in 100 μg of whole cell extract as measured by immunoblots. The overall yield is estimated to be approximately 25 percent.

J. Côté and J. L. Workman are in the Department of Biochemistry and Molecular Biology and the Center for Gene Regulation, The Pennsylvania State University, University Park, PA 16802, USA. J. Quinn and C. L. Peterson are in the Program in Molecular Medicine and the Department of Biochemistry and Molecular Biology, University of Massachusetts Medical Center, Worcester, MA 01605, USA.

---

*To whom correspondence should be addressed.